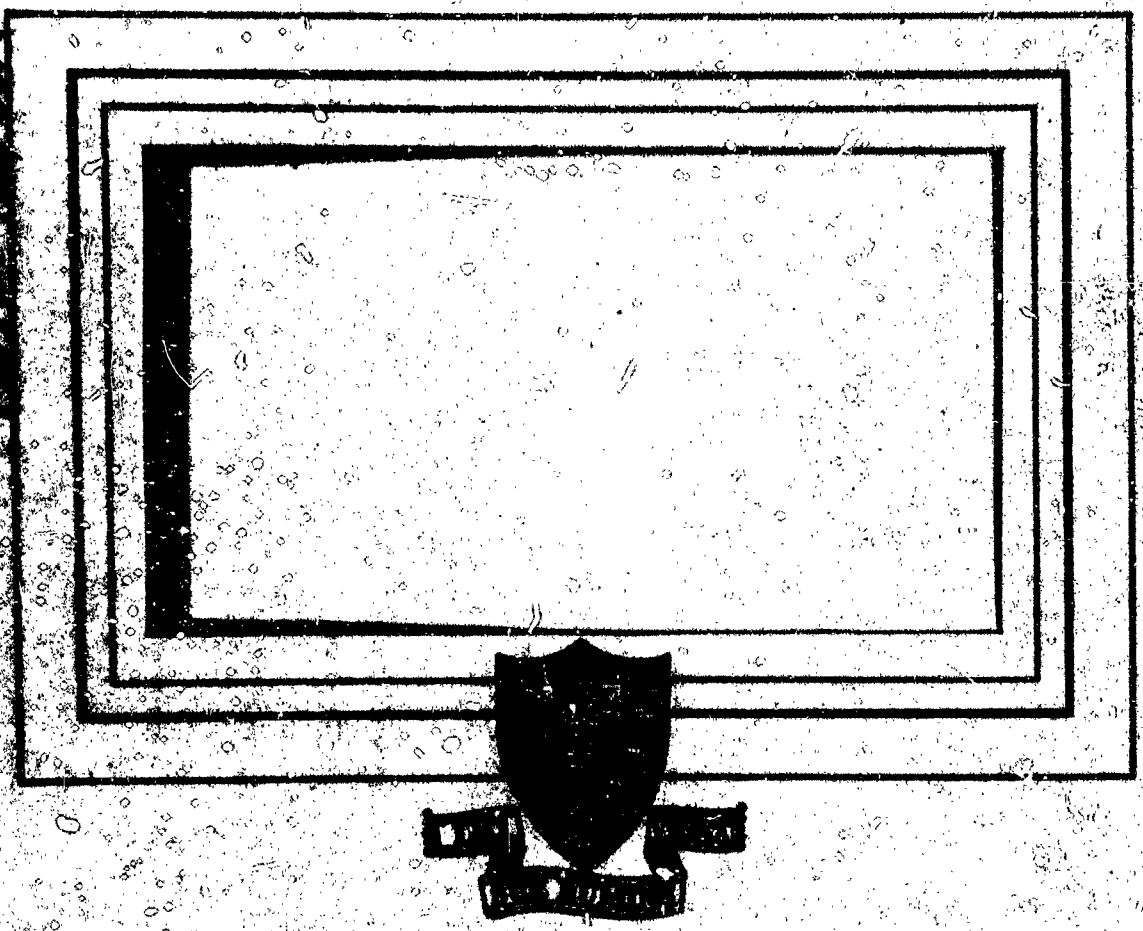

RESEARCH BULLETIN

THE JAMES FORRESTAL RESEARCH CENTER
PRINCETON UNIVERSITY

OFFICE OF NAVAL RESEARCH
Contract N6 onr-27015
Project NR 212-005

A REVIEW OF ROTOR INDUCED VELOCITY FIELD THEORY

Aeronautical Engineering Department

Report No. 248

January, 1954

Prepared by: Robin B. Gray
ROBIN B. GRAY

Approved by: A. A. Nikolsky
A. A. NIKOLSKY

Summary

A review of all the currently available papers concerned with the solution of the problem of the induced velocity field of a helicopter rotor is presented. The assumptions, applications, and limitations of each paper are given. Since, in general, all the theories are very limited in their applicability, it is recommended that further theoretical and experimental investigations be initiated which will be directed toward a more accurate prediction of the induced velocity field about a rotor.

2.

Introduction

Although the concept of the lifting rotor is quite old, it has not been until recently that the special problems involving the air flow through and around such a rotor have been theoretically and experimentally investigated. In fact, in general, such investigations were necessarily delayed until the successful flight of a lifting rotor in various regimes began to point out control and vibrational difficulties which were obviously brought about by the variation in the rotor inflow velocities. The theories available were merely extensions of the propeller theories whose origin, except for the vortex concept, lay in the older marine screw theories. While these momentum, blade element, and vortex theories are adequate for performance estimation, they are woefully inadequate for use in predicting blade motions for stability and control, vibration, and blade stress problems. This is particularly true at slow forward flight speeds and vertical descent.

The purpose of this review then is to trace the development of the rotor induced velocity field theory, to present the applicability and limitations of each theory, to reach a conclusion concerning the state of the knowledge and to point out, if possible, ways and means of improving or extending the theory.

This review is divided into four main parts as follows: momentum theory, blade element theory, combined momentum and blade element theory, and vortex theory. The development of each concept is treated chronologically from its beginning to its present state. Since the investigations and theoretical analyses of marine screws, propellers, and rotors prior to 1935 are adequately presented and referenced by H. Glauert in reference 1, this work is the primary source for material prior to that year. Thereafter, only the individual papers that dealt solely with rotors and their special problems are reviewed.

This literature review of rotor induced velocity field theories was carried out at Princeton University under the sponsorship and with the financial assistance of the Office of Naval Research.

It might be well to briefly review the various flight regimes of the helicopter before starting the review. There are three basic flow patterns. The first corresponds to the propeller working state and includes hovering, horizontal, and ascending flight. In these flight regimes, the air at a great distance ahead of the rotor and the air passing through the rotor in general proceed in a downward direction with respect to the tip-path plane. The second flow pattern is designated the windmill-brake state. This corresponds to a flight condition in which the rotor is disconnected from the engine and is driven by the air passing through it. In this case, the air at a great distance ahead of the rotor and the air passing through the rotor proceed in an upward direction with respect to the tip path plane. The third flow pattern lies between the first two. This corresponds to certain portions of the descending flight regime and is called the vortex-ring state. Rotor operation in this state is usually very rough. The air at a great distance ahead of the rotor is moving upward while the air passing through the rotor disk is moving downward with respect to the tip path plane. The limiting condition between the vortex-ring and the windmill-brake states is called the ideal autorotation condition in which very little air passes through the disk. The limit between the propeller-working and vortex-ring states in vertical flight is of course the hovering condition. In forward flight this limit will lie along some descending flight path since the tip path plane is usually inclined forward.

4.

List of Symbols

Throughout this paper an effort was made to use as many as possible of the standard symbols for helicopters as set forth in reference 2. This necessitated the replacement of some of the symbols in some of the papers reviewed with these standard symbols. In some cases, however, this was not feasible and some duplication exists. In these cases, the symbol is defined where used, and it is hoped that no confusion will arise.

a	slope of lift curve for blade element, per radian (blade element section)
a	axial interference factor, $U_p = V_r (1 + a)$ (momentum section)
a'	rotational interference factor, $u' = 2a'\Omega$
a_{1_s}	longitudinal angle between the rotor shaft and the perpendicular to the tip path plane, radians
b	number of blades in rotor
c	blade chord at radius r
c_{d_o}	section profile - drag coefficient
c_l	section lift coefficient
C_T	rotor thrust coefficient $\frac{T}{\rho \pi \Omega^2 R^4}$
C'_T	rotor thrust coefficient based on flight velocity $\frac{2T}{\pi R^2 \cdot \rho V^2}$
K	non-dimensional function f $(\varphi, \frac{r}{R}, b)$ in Goldstein vortex theory
L	lift, pounds
p	static pressure, pounds per square foot
P	power, foot-pounds per second
Q	rotor torque, foot-pounds
r	radius of blade element from rotor center, feet
R	radius of rotor blade tip, feet
R_1	radius of ultimate rotor wake, feet
s	gap distance between vortex sheets forming wake, feet

T rotor thrust, pounds

u' rotational component of wake velocity, radians per second

U component of resultant velocity at blade element that is normal to blade axis, feet per second

U_P component of resultant velocity at blade element that is normal to blade span axis and U_T, feet per second

U_{P_1} component of resultant velocity in ultimate wake that is normal to a plane parallel to tip path plane, feet per second

U_T component of resultant velocity at blade element that is normal to blade-span axis and to axis of no-feathering, feet per second

v normal component of induced velocity at tip-path plane, feet per second

$\underline{v}$ vector sum of the three components of induced velocity, feet per second

v_o average value of fore-and-aft induced velocity at the center of the disk, feet per second

$\dot{v}_o$ rate of change of induced velocity at center of disk, feet per second

v_r radial component of velocity induced at a point P by a vortex ring, feet per second

v_z axial component of velocity induced at a point P by a vortex ring, feet per second

$v''_{z_{\frac{3}{4}R}}$ axial component of induced velocity at 3/4 radius due to bound vortices, feet per second

v'''_{z_o} axial component of induced velocity at rotor center due to Γ_o component of the free tip vortices, feet per second

$v'''_{z_{\frac{3}{4}R}}$ axial component of induced velocity at 3/4 radius due to Γ_o component of the free tip vortices, feet per second

$v''''_{z_{\frac{3}{4}R}}$ axial component of induced velocity at 3/4 radius due to the free-radial and tip vortices, feet per second

V true airspeed of helicopter along flight path, feet per second

V_V component of true airspeed of helicopter normal to tip path plane, feet per second

w rotational component of induced velocity, feet per second

W gross weight of helicopter, pounds

$2W'$ velocity of axial translation of the rigid helicoidal surface, feet per second

6.

x ratio of blade-element radius to rotor-blade radius, r/R

α_1 attitude angle of fuselage; angle between rotor axis and the vertical, radians

α_r blade-element angle of attack measured from line of zero lift, radians

α_s angle between the slipstream and the perpendicular to the tip-path plane at the rotor disk, radians

α_T angle of attack of tip-path plane measured in the longitudinal plane between the flight-path velocity vector and tip-path plane, radians

Γ circulation of blade element at radius r and azimuth angle

Γ_0, Γ_1 constants in expression for Γ $\quad (\Gamma = \Gamma_0 - \Gamma_1 \sin \psi)$

ϵ ratio of profile-drag coefficient to lift coefficient $\frac{c_{d_0}}{c_l}$

η propeller efficiency

θ blade pitch angle at particular blade radius and azimuth position, radians

κ coefficient in Goldstein vortex theory as modified by Lock which represents the circulation loss along the blade

μ_T in-plane velocity ratio at tip path plane $\frac{V \cos \alpha_T}{\Omega R}$

ρ density of air, slugs per cubic foot

σ_r rotor solidity at radius, r

φ inflow angle at blade element measured in plane perpendicular to blade axis and between tip-path plane and relative wind, radians

φ_1 angle that the helical surfaces of the vortex sheets make with the propeller disk plane, radians

Φ_p potential at a point P due to a closed vortex ring

χ wake skew angle, angle between perpendicular to tip path plane and wake boundary at a far distance below the rotor disk in a longitudinal plane, radians

ψ azimuth position of blade measured from downwind position in direction of rotation, radians

ω solid angle subtended at a point by a vortex ring

Ω rotor angular velocity, radians per second

Subscript - r, unless otherwise noted, denotes radial position on blade

Momentum Theory

The simple axial momentum theory as first originated by W. J. M. Rankine in 1865 (reference 3) was based on the concept that the forces experienced by a set of rotating blades immersed in a frictionless, incompressible fluid were equal to that necessary to provide the resulting motions of the fluid. In further simplifying the physical picture, it was assumed that the slipstream had no rotational component, that the thrust of the propeller was constant over the disk, that the axial velocity of the fluid had a constant value over the disk and over a cross-section of the ultimate wake, and that the resultant pressure force on the whole fluid was zero. Then assuming the propeller to be at rest and the fluid to have a uniform velocity along its axis, the thrust on the propeller was equated to the axial increase in momentum in unit time, so that

$$T = \pi R_1^2 \rho V_{p_1} (V_{p_1} - V_v)$$

where the subscript 1 refers to the ultimate wake. Since the propeller was assumed to be at rest, no useful work was done and the power absorbed was taken as being equal to the increase in kinetic energy of the slipstream in unit time, so that

$$\Delta K.E. = P = \tfrac{1}{2} \pi R_1^2 \rho V_{p_1} (V_{p_1}^2 - V_v^2)$$

Then using the condition of continuity of flow, it was shown that

$$V_p = \tfrac{1}{2} (V_{p_1} + V_v)$$

This was one of the most important features of the momentum theory. It pointed out that the axial velocity of the fluid moving through the propeller disk was greater than the forward velocity of the disk. It further showed that the induced velocity at the disk was one-half its value in the ultimate

8.

wake. This result may also be obtained by a suitable application of Bernoulli's equation, the continuity equation, and the axial momentum equation. The efficiency of propulsion was then shown to be

$$\eta = \frac{T V_v}{P} = \frac{2 V_v}{U_p + V_v}$$

By introducing an axial interference factor a, where

$$U_p = V_v (1 + a)$$

it was shown that the ideal propeller efficiency became

$$\eta = \frac{1}{(1 + a)}$$

which is the highest efficiency that can be obtained from a propeller of given disk area, velocity of advance, and power absorption. A consequence of this relation was that the minimum loss of energy for a given thrust occurred when the thrust was uniformly distributed over the whole disk. This distribution maintained a constant value of the axial interference factor.

R. E. Froude, in 1889 (reference 4) introduced the actuator disk concept. This concept represented the propeller as a disk at which there is a sudden increase in pressure without a discontinuity in velocity. This may be physically represented by considering a close pair of contra-rotating coaxial propellers having an infinite number of frictionless blades so designed that the rotational velocity component of the front propeller is exactly cancelled by the component of the rear for each radial annulus, and that the blade angles are chosen in such a manner as to yield a uniform distribution of thrust over the disk.

N. E. Joukowski, in 1918 (reference 5), and A. Betz, in 1920 (reference 6), extended the axial momentum theory to the more general case by taking the rotational velocity component into account. A similar derivation is given by H. Glauert, (reference 1). It was assumed that the actuator disk introduced a

rotational component to the fluid velocity while the axial and radial component remained unchanged. This further generalization of the theory resulted in equations which were rather difficult to solve, unless the wake angular velocity component was known as a function of the radius. Thus, an exact solution could be realized when the flow in the slipstream was assumed to be irrotational except along the axis. This assumption implied that the rotational momentum had the same value for all radial elements and further that the circulation along the blade was constant. Such a distribution was not physically realizable since it would mean that close to the axis the wake had a greater angular velocity than the blade itself. Consequently the blade was usually assumed to begin at the radial station at which the angular rotation imported to the slipstream was identical to the rotational velocity of the blade itself. For this particular case it was shown that when rotation of the slipstream was taken into account, the induced velocity at the disk was not necessarily one-half its value in the ultimate wake. In fact

$$U_p > \tfrac{1}{2}(U_{p_1} + V_r)$$

In general since the angular velocity imported to the slipstream was very much smaller than the angular velocity of the propeller blades, it was possible to simplify the general equations by neglecting certain terms involving the square of the wake rotational component. This yielded results similar to the simple axial momentum theory for the relationship connecting the thrust and axial velocity. The equations for the thrust and torque of an ideal frictionless propeller are given on page 196 of reference 1 and are as follows:

$$dT = 4\pi\rho V_r^2 (1+a)\, a\, r\, dr$$

$$dQ = 4\pi\rho V_r \Omega (1+a)\, a'\, r^3 dr$$

where a, the axial interference factor, is defined by

$$U_p = V_p(1+a)$$

10.

and a', the rotational interference factor, is defined by

$$u' = 2a'\Omega$$

where u' is the wake rotational component. The factors a and a' are related by the expression

$$V_r^2(1+a)a = \Omega^2 r^2 (1-a')a'$$

The efficiency for this case is

$$\eta = \frac{1-a'}{1+a}$$

The condition for minimum loss of energy when the slipstream rotation was included, neglecting second order and higher small quantities, was for a distribution of thrust such that the efficiency had the same value for all elements. This simple condition applied only to lightly loaded propellers.

The momentum theory may be extended to include frictional drag of the blades and the interference of nearby bodies. Rankine, in reference 3, gave an estimate of these effects.

The great disadvantage of the momentum theory was that it gave no indication of the manner in which the blades should be designed, other than that the diameter of the propeller should be as large as possible.

A classical approach to the problem has been given by Mangler in references 7, 8, and 9. He also used the actuator disk concept in which the rotor was replaced by a circular disk with a pressure step across it. This implied a rotor having an infinite number of blades but was a good assumption if the rotor blades were driven at a high angular velocity. A second assumption was made in which it was assumed that the rotor was either lightly loaded or that the velocity along the flight path was large so that the induced velocities were small compared to the flight path velocity. It was also assumed that the induced velocities that were associated with the rotor torque could be neglected. The second assumption allowed the author to use the linearized theory as explained

by Burgers in reference 10. The Euler Equations could then be simplified so that only linear terms were retained:

$$-V \frac{d\underline{v}}{dx} = -\frac{1}{\rho} \text{ GRAD } p$$

where $\underline{v}$ is the vector sum of the three components of induced velocity and p is the static pressure. Since the continuity equation had to be satisfied, i.e.

$$\text{div } \underline{v} = 0$$

it was shown that

$$\text{div GRAD } p = \nabla^2 p = 0$$

The static pressure function was therefore a potential function and the acceleration, $-V \frac{d\underline{v}}{dx}$ was the gradient of this potential function. Then by integrating the first equation above it was shown that

$$\frac{\underline{v}}{V} = \frac{1}{\rho V^2} \int_{+\infty}^{x} \text{GRAD } p \, dx$$

The lower limit was taken as $+\infty$ since the induced velocities must vanish at a far distance ahead of the rotor and the integration was performed for constant y and z . This result applied everywhere but inside the wake since the integration could not be performed across the disk. However, it was explained that since the integrated equation was everywhere continuous outside the disk and wake, the analytical continuation of this expression could be used inside the wake if another function $\underline{f}(r, z)$ were added to it to make the velocity continuous across the disk. Thus for the space within the wake

$$\frac{\underline{v}}{V} = \frac{1}{\rho V^2} \int_{+\infty}^{x} \text{GRAD } p \, dx + \underline{f}(r, z)$$

The wake was not, however, irrotational and a velocity discontinuity existed at the wake boundaries.

Mangler's solution of the Laplace equation

$$\nabla^2 p = 0$$

12.

followed that of Kinner in reference 11. This latter paper was originally intended as a contribution to the theory of the autogiro, but, in order to limit its scope and due to mathematical difficulties, was restricted to the problem of the solid flat circular disk. Mangler in a manner similar to Kinner solved the Laplace equation in terms of Legendre functions of the elliptic coordinates of the rotor disk (i.e. ellipsoidal harmonics). These functions were discontinuous between the two faces of the disk but were continuous everywhere else. It was then possible to solve the induced velocity integral equation but this was difficult and lengthy even for simple distributions. The solution was then restricted to axially symmetric pressure distributions in which the load was a function of disk radius only and not blade azimuth position. Three pressure distributions were used. The first term of the series of Legendre functions gave an elliptical distribution and the thrust. The second term gave a moment but this term was not used. The third term when combined linearly with the first term in a suitable manner gave a pressure distribution which was zero at the center and circumference of the rotor disk and was a reasonable approximation for the load existing on a rotor in forward flight. The first and combined first and third pressure distributions were the ones used in the report for the calculation of the induced velocity perpendicular to the disk and the vertical induced velocity at a point far behind the disk. These calculations were tabulated and plotted for rotor angles of incidence of 0, 15, 30, 45, and 90 degrees.

The results of these calculations showed that the induced velocity distribution over a rotor disk was far from constant or a linear variation. Within the limitations of the theory and for the angles of incidence within the realm of possibility for a helicopter in forward flight, the induced velocity for the first pressure distributions was directed upward at the front

and sides and downward over the remainder of the disk. For the combined first and third pressure distributions, several maxima and minima existed on the disk. The induced velocity was directed upward at the front and sides of the disk and downward at the rear but another area of up flow existed just to the rear of the center of the disk. The induced velocity at the center of the disk was equal to zero and was independent of the angle of incidence of the rotor. It was found that the local peaks in the upwash could be removed by fairly small alterations of the load distribution.

At large distance behind the rotor the vertical component of the induced velocity was directed downwards near the middle and upwards on both sides and was symmetrical with respect to the plane $z = 0$. There was a singularity at the wake boundary.

In reference 9, the Fourier series representation of the downwash distributions for the two previously mentioned pressure distributions were given in terms of the azimuth angle, rotor radius, thrust coefficient, flight path velocity, and rotor angle of incidence. Only pressure distributions having lateral symmetry were considered. This Fourier representation makes the calculation of the blade motion more convenient. The Fourier series could also be used to determine numerical values of the downwash distribution over the disk, except at points near the circumference at zero incidence.

The authors stated in reference 7 that the assumption that the induced velocities were small compared to the flight path velocity "implies a serious limitation in the applicability of the results." To define the limits of applicability, the following criterion was established.

$$C_T' = \frac{T}{\pi R^2 \cdot \frac{1}{2}\rho V^2} = \frac{2 C_T \cos^2 \alpha_V}{\mu_V^2} << 1$$

No indication was given, however, as to the order of smallness required to

fulfill this criterion. For present day helicopters, the value of this coefficient falls in the range of about 1/5 to 1/12 with the cruising speeds falling toward the high end of the range and the maximum speed falling toward the low end.

In conclusion, the authors stated that a sound mathematical theory had been constructed for the induced velocity field of a rotor within the limitations of the assumptions. They further stated that there should be no fundamental difficulty in extending the theory to unsymmetrical load distributions which occur in practice.

An attempt was made by P. Brotherhood and W. Stewart, in reference 12, to compare the variation in induced velocity along a fore and aft chord of the rotor disk as calculated by the theory with the results of a full scale flight test of an R-4B. The elliptical load distribution was used in the theoretical calculation for both 0 and 15 degrees angles of incidence of the rotor. It was found that in general, this distribution resulted in values which were higher (both positively and negatively) than the measured values, particularly over the aft portion of the disk. The measurements were made for μ_v's of 0.138, 0.167, and 0.188. The agreement was somewhat better at the higher flight speeds than at the lower, indicating possibly that the limitations of the analysis were being exceeded.

In reference 13 by Daughaday and Kline the experimental data indicated the presence of some large periodic forces exciting the first, second, and third bending modes of the rotor blades at multiples of from three to ten times rotor RPM. These results were in complete contradiction with the theory which showed that the exciting forces above two per revolution should be negligible. Since the theory had assumed a uniform downwash, it was decided to use Mangler's downwash analysis to calculate the generalized forces. The combined first and

third pressure distributions were used in the calculation. The results of this analysis, according to reference 13, indicated that the variation in induced velocity was probably the primary source of the higher order excitation. It was further stated that the theory was not sufficiently refined to be used exclusively in rotor blade design, in that the designer must still exercise considerable judgement in the selection of generalized forces.

Fail and Eyre, in reference 14, made some downwash measurements behind a 12-foot helicopter rotor in a wind tunnel under simulated forward flight conditions. The measurements were made in a vertical plane 1.5 rotor radii behind the rotor center at four spanwise locations. In comparing the theory and experiment, an allowance must be made for the displacement of the rotor wake since the first order theory excluded such a displacement. In computing the theory, reasoning seemed to indicate that the first or elliptic blade spanwise pressure distribution would most nearly approximate the loading on the advancing blade, while the combined first and third terms of the Legendre function, which gave a pressure distribution that was zero at the rotor center and tip, would more nearly approximate the loading on the retreating blade. In general, it was found that the experimental data approximately corresponded to the above reasoning. In some instances the agreements between theory and experiment were quite good if allowance was made for the wake displacement. In other cases the agreement was not good. There appeared to be no correlation between μ_V, α_V, and spanwise location and the agreement or disagreement of the comparison. In fact, some of the better agreements corresponded to flight conditions which violated the limitation that $C_T' << 1$. No measurements or comparisons were made for the plane of the rotor blades.

16.

Blade Element Theory

The simple blade element theory was originally introduced by W. Froude in 1878 (reference 15). This theory considered in a crude form, the forces experienced by the blades as they moved through the air. S. Drzewiecki, beginning about 1892 (references 16 & 17), took up the development of this concept and later published a complete analysis of the theory (reference 18). The analysis was based on the premise that a propeller blade may be considered as made up of many airfoil elements of small span advancing along a helical path determined by the axial velocity and the rotational velocity of the propeller. Its great advantage was that it yielded the blade geometry but had the disadvantage that it required the experimental determination of the airfoil characteristics and arbitrary assumptions as to the effective aspect ratio. At this time and for a considerable period thereafter there was much uncertainty as to what airfoil characteristics should be used. Drzewiecki proposed to determine the airfoil characteristics and interference effects by a series of tests on a number of special propellers.

F. W. Lanchester, along with his airfoil theory, developed a blade element theory for propellers in 1907 (reference 19). He attempted to account for the mutual interference effects by an anology with an infinite staggered cascade of airfoils.

The basic assumption of these theories has been that the blade element between a radius r and r + Δ r of a propeller advancing along its axis with a uniform velocity and rotating about this axis with a uniform angular velocity, was considered to be an airfoil element of the same cross-section advancing through the air with a uniform linear velocity which was the resultant of the axial and rotational velocities and at an angle of incidence, α_γ .

Consequently, the aerodynamic force acting on the blade element was the same as that acting on the aforementioned fictitious airfoil. Then the total force acting on the blade was the sum of that acting on each individual blade element. It was assumed that there was no mutual interference between blade elements except as the interference modifies the characteristics of the blade elements. According to these primitive blade element theories, the equations representing the complete solution of the behavior of a propeller are

$$\frac{dT}{dr} = \frac{1}{2} b c \rho U^2 (c_l \cos\varphi - c_{d_o} \sin\varphi)$$

$$\frac{dQ}{dr} = \frac{1}{2} b c r \rho U^2 (c_l \sin\varphi + c_{d_o} \cos\varphi)$$

where

$$\tan\varphi = \frac{U_P}{U_T}$$

$$c_l = a(\theta - \varphi)$$

$$c_{d_o} = \delta_o + \delta_1 \frac{c_l}{a} + \delta_2 \left(\frac{c_l}{a}\right)^2$$

These equations must be graphically integrated for the general case.

The formula for the efficiency of the blade element is

$$\eta = \frac{1 - \varepsilon \tan\varphi}{1 + \varepsilon \cot\varphi}$$

where $\varepsilon = \frac{c_{d_o}}{c_l}$. Solving for the maximum efficiency, disclosed the fact that according to the blade element theory, the efficiency of a propeller decreased as the diameter increased above a certain optimum value which was an absolute contradiction of the conclusion reached by the ideal momentum theory.

Another difficulty was that these theories predicted that the thrust and torque of a given propeller at a given advance ratio should vary directly as the number of blades, a fact which experimental investigations had definitely disproved. The conclusion which these discrepancies indicated was that the primitive blade element theory did not give a complete and satisfactory answer as regards to the behavior of the propeller.

18.

Combined Momentum and Blade Element Theories

It was pointed out in the previous section that while the blade element theory predicted the observed performance of propellers in a general way, it failed to give accurate numerical results. In an attempt to reconcile the theory with experimental results, each of three of the basic assumptions were critically examined. (See reference 1, page 215).

The first assumption considered was the independence of blade elements, i.e. that the force on an airfoil element was not affected by the forces on adjacent elements of the same blade. This fact could not be established rigorously but the effect was believed to be quite small. However in order to dispel all doubt, a series of experiments were undertaken by C. N. H. Lock, around 1924 (reference 20), by which the independence of blade elements was verified.

The next assumption to be considered was that the effective velocity of the blade through the air was the resultant of the propeller axial and rotational velocity. In both England and Germany, it was proposed that the increase in axial velocity of the air at the propeller disk as predicted by the momentum theory should be included in the blade element theory. H. Reissner, in 1910, (reference 21) was the first who tried to combine the momentum theory and the blade element theory. A. Betz in 1915, (reference 22) and G. de Bothezat about 1918 (reference 23) included in their blade element theories, this increased axial velocity of the air as determined by the ideal momentum theory. In England, however, A. Fage and H. E. Collins, in 1917, (reference 24) proposed that an empirical estimate of the increased axial velocity of the air be included. This latter theory was extended to include the rotational component by L. Bairstow (reference 25). Another approach to the problem was made by

R. McK. Wood and H. Glauert, in 1918, (reference 26). They used Lanchester's concept (reference 19) which proposed that the mutual interference of propeller blades was analogous to that of a staggered cascade of airfoils. Drzewiecki (reference 18) maintained that the increase in axial velocity of the air at the propeller disk as determined from momentum theory was only an average of a periodic flow and therefore should not be used in estimating the force experienced by the blade element.

The third assumption was concerned with what airfoil characteristics should be used. All of the previously mentioned blade element theories suffered from this assumption. Betz, in reference 22, indicated that the aspect ratio of the propeller blades tended to be infinite but depended also on the blade shape. Fage and Collins, in reference 24, used an aspect ratio of 6 and attempted to correct the theory by an empirical inflow velocity. Drzewiecki and de Bothezat proposed special propeller tests to determine the required airfoil characteristics. The main difficulty was that the variation of the airfoil characteristics with aspect ratio was still undetermined at that time, both from a theoretical and experimental viewpoint.

H. Glauert in 1922, (reference 27) developed a combined axial momentum and blade element theory in which he indicated that to be consistent with the assumption of the independence of blade elements, the airfoil characteristics must be taken from tests in which the airfoil elements experienced no interference from adjacent elements, that is, infinite aspect ratio tests. This analysis was later extended to the case of the helicopter by Glauert (reference 28, 29, and 30), C. N. H. Lock, (reference 31), H. B. Squire (reference 32) and many others. These references gave essentially the same analysis which is used today for helicopter performance and design.

20.

After the first successful flight of a helicopter, it became obvious that these theories and their assumptions were not adequate for predicting the various vibrations and blade motions encountered. In attempting to refine the theories, the attack was directed toward finding a theoretical method of predicting the variation of the induced velocity across the rotor disk which was more realistic.

Several authors have made use of the combined momentum and blade element theory in this field with some success. R. S. Ross (reference 33) set up the general equations determining the airflow beneath helicopter rotors using these classical concepts as applied to an elementary disk annulus. An expression was obtained for the blade span loading in terms of the local induced velocity and the local lift-drag ratio. For hovering the expression became

$$\frac{c_l b c}{r} = \frac{17.77\, D^2}{\left[1 - \varepsilon D + \sqrt{1 - 2\varepsilon D - D^2}\right]^{3/2}}$$

where $D = \frac{2V}{\Omega r}$

$\varepsilon = \frac{c_{do}}{c_l}$

In order to solve this equation, three charts were prepared as follows: 1. the particular airfoil characteristics, c_l and ε versus angle of attack; 2. a plot of the design coefficient $\frac{c_l b c}{r}$ or span loading versus $\frac{2V}{\Omega r}$ for various lift-drag ratios, 3. a plot of inflow angle φ versus velocity ratio $\frac{2V}{\Omega r}$ for various lift-drag ratios. Then by assuming several values of c_l, a value of the local induced velocity could be determined from the intersection of two c_l versus $\frac{2V}{\Omega r}$ curves for the particular radius. The rotational component, u', could then be determined from the equation

$$u' = (\Omega r - \varepsilon V_v)\left[1 - \sqrt{1 - \frac{4V^2 + 4VV_v + 4\varepsilon V \Omega r}{\Omega r - \varepsilon V_v}}\right]$$

Actual velocity measurements were made with a hot wire anemometer underneath a model rotor in hovering flight and compared with theory. In general good results were obtained over the inboard center portion of the blade for both velocity components but comparison was poor toward the tips and close to the root.

The design formula was modified to account for horizontal flight with the rotor horizontal and then further modified to include either hovering, vertical, or horizontal flight. Although velocity measurements were also made for the horizontal flight conditions, there was no comparison with theory. Flight records indicated the pulsations or periodicity of the flow that occur in horizontal flight.

W. Castles and A. L. Ducoffe (reference 34) derived an expression for the distribution of the induced velocity across a rotor disk in hovering flight as a function of the thrust at that radius and of a semi-empirical constant, k, to account for the viscous shearing force in the flow. The thrust on an elemental annulus as determined from momentum considerations was equated to the lift on the portion of the blades lying within the annulus as determined by blade element considerations. This yielded an induced velocity distribution.

$$v_r = \frac{\Omega r}{\cos \alpha_s} \sqrt{\frac{\sigma_r c_{l_r} k}{8}}$$

where α_s is the wake angle of each annulus stream tube at the disk. Using this value of the induced velocity, the induced angle of attack of the blade was determined. Then using the relation $c_{l_r} = a(\theta_r - \varphi_r)$ and the determined relationship $\varphi_r = \sqrt{\frac{\sigma_r c_{l_r} k}{8}}$, the local lift coefficient for each blade element could be determined. The thrust and torque integral equations were then set up for any twist, taper, or planform. These integrated equations gave results which were in good agreement with the available experimental data. The factor k was determined empirically from experimental data. A similar analyses

22.

was made for hovering within ground effect.

As pointed out in the previous section there were several inconsistances and contradiction between the ideal momentum theories and the blade element theories. One inconsistancy was that in direct opposition to the ideal momentum theory which indicated an upper limit to the efficiency of a propeller depending only on the disk loading for a given advance ratio, the blade element theory indicated that the efficiency approached 100% as the drag of the blade approached zero. Furthermore, the primitive blade element theory indicated that the efficiency of a propeller decreased as the diameter increased above a certain optimum value which was an absolute contradiction of the ideal momentum theory which indicated that the efficiency should increase with diameter for a given thrust. The rigorous reconciliation of these two theories awaited the development of the vortex theory.

Vortex Theory

The fundamental bases of the vortex theory were the Lanchester-Prandtl-Joukowski conception of the vortex system, the Kutta-Joukowski theorem, and Prandtl's airfoil theory. The Kutta-Joukowski theorem stated that the lift of an airfoil was determined by the circulation existing about its contour. That is, that the lift per unit length of span in a two dimensional flow was given by the product of the circulation Γ about its contour, the density ρ of the fluid, and the uniform velocity V of the airfoil through the fluid, namely

$$L = \rho V \Gamma$$

The concept of this circulation about the blade led to the concept of the bound vortex or lifting line and as a consequence to the free vortices which are shed by the blade and pass down stream in a helical pattern forming the slipstream. This type of slip-stream configuration was apparently first recognized by F. W. Lanchester around 1900 and was later published in 1907 in reference 19. N. E. Joukowski investigated the induced velocity resulting from this type of vortex system in 1912 (references 5 and 35) but in order to reach a solution was forced to assume that the blades were lightly loaded and of infinite number. This resulted in a theory identical to the momentum theory as to the axial and rotational induced velocities but Joukowski went further and suggested using an infinite aspect ratio cascade of airfoils to obtain the required airfoil characteristics.

A. Betz, in 1919 (reference 36), applied Prandtl's elliptic loading airfoil theory and showed that a propeller of given thrust and power had a minimum loss of energy and highest efficiency if the shed vortex sheets after an initial limited distortion, moved backward as a rigid screw surface (i.e. constant

24.

axial velocity). The application of this theory to a propeller was not simple, but the problem was capable of being solved if the propeller was assumed to have an infinite number of lightly loaded, frictionless blades. L. Prandtl, in an addendum to reference 36, indicated an approximate method for correcting the results for a propeller with a finite number of blades. In this case instead of a uniform distribution of vortex sheets implying no gap, there was now a system of vortex sheets with a gap, s , depending upon the angle φ_1 of the screw surface at the boundary of the slipstream.

$$s = \frac{2\pi R}{b} \sin \varphi_1$$

where $\tan \varphi_1 = \frac{V_r}{\Omega R}$ and b is the number of blades. Whereas before there was zero slipstream contraction and the radial velocity component was negligible, there is now an appreciable radial velocity at the boundary of the slipstream as the air attempts to flow around the edges of the vortex sheets. Prandtl replaced these vortex sheets by a system of semi-infinite plane surfaces of zero thickness and gap, s , equal to that of the actual vortex sheet. The flow about this system of planes was determined for the case of a uniform motion downward at right angles to the planes. Using the solution to this system, the flow about the vortex sheets could be approximately estimated. A graph of the approximate correction factor as a function of the number of blades and advance ratio is given on page 263, reference 1. S. Goldstein has developed a more accurate analysis of the problem of a finite number of blades by the use of Bessel functions (reference 37). This was a rigorous solution of Betz's optimum condition but assumed zero slipstream contraction. Hence it is directly applicable only to lightly loaded propeller. Goldstein's method has been extended to the general case by Lock, reference 38. These theories are applicable to a helicopter rotor only for the special cases of hovering flight and vertical ascent. A brief summary of Lock's theory will be given here.

A more complete form of the derivation may be found in reference 39.

Goldstein showed that the circulation distribution along the blades of a propeller was (according to his assumptions)

$$\Gamma = \frac{2 W' K \, 2\pi r \, \tan \varphi_1}{b}$$

where $2W'$ is the velocity of axial translation of the rigid helicoidal surface; K is a non-dimensional function φ_1, the ratio $\frac{r}{R}$, and the number of blades b, and φ_1 is the angle that the helical surfaces make with the propeller disk plane. It was then shown that

$$2W' = \frac{2V}{\cos^2 \varphi_1}$$

and hence

$$\Gamma = \frac{2V K}{\cos^2 \varphi_1} \cdot \frac{2\pi r \, \tan \varphi_1}{b}$$

Lock replaced the factor $\frac{K}{\cos^2 \varphi_1}$ by a new coefficient $\mathcal{K}$ which represented the circulation loss along the blade. Thus

$$\Gamma = \mathcal{K} \cdot \frac{4\pi r V \, \tan \varphi_1}{b}$$

Using the Kutta-Joukowski theorem that

$$\Gamma = \tfrac{1}{2} c_l c U$$

and solving for the axial induced velocity, v, gave

$$v = \frac{b c c_l U}{8\pi r \mathcal{K} \tan \varphi_1}$$

The rotational component was then

$$w = \frac{v}{\cos \varphi_1}$$

The expression for the distribution of thrust and torque along a single blade were

$$\frac{dT}{dr} = \tfrac{1}{2} \rho c U^2 (c_l \cos \varphi_1 - c_{d_0} \sin \varphi_1)$$

$$\frac{dQ}{r dr} = \tfrac{1}{2} \rho c U^2 (c_l \sin \varphi_1 + c_{d_0} \cos \varphi_1)$$

26.

The solution of these equations required that a value of φ_1 be assumed for each blade station considered and by trial and error, finding the distribution of φ_1 which gives the desired integrated value for the thrust. This is at best a rather complicated solution though the results compare very well with experiments.

M. Knight and R. Hefner, in 1937 (reference 40), using a vortex system similar to that of Joukowski (reference 5) and Glauert (reference 27) applied this concept to the lifting rotor. The basic assumptions employed were the same as those of the latter two references and were as follows: the number of blades was taken as infinite; the induced angles were small so that the sine and tangent were equal to the angle itself in radians; and the rotational and radial components of velocity, tip losses, and slipstream contraction were neglected. Each blade was replaced by a rotating lifting line. The trailing vortices which sprang from the tips formed a helix in space while the vortices from the root became concentric with the axis of rotation and were neglected. The problem thus was reduced to finding the normal component of the velocity which was induced at the rotor disk by a cylindrical surface of vorticity.

In order to simplify the analysis, the helical pattern of vorticity was broken up into two simpler patterns. One was composed of circular vortex rings and the other of axial vortex lines, both together forming a right circular cylinder of vorticity extending from the rotor disk downward to infinity. However in this analysis, the latter pattern was neglected. The analysis makes use of the fact that the potential Φ_p at a point P due to a closed vortex ring is directly proportional to the product of the circulation Γ' and the solid angle ω subtended by the vortex ring at P.

$$\Phi_p = \frac{\Gamma'}{4\pi}\omega$$

26.

The solution of these equations required that a value of φ_i be assumed for each blade station considered and by trial and error, finding the distribution of φ_i which gives the desired integrated value for the thrust. This is at best a rather complicated solution though the results compare very well with experiments.

M. Knight and R. Hefner, in 1937 (reference 40), using a vortex system similar to that of Joukowski (reference 5) and Glauert (reference 27) applied this concept to the lifting rotor. The basic assumptions employed were the same as those of the latter two references and were as follows: the number of blades was taken as infinite; the induced angles were small so that the sine and tangent were equal to the angle itself in radians; and the rotational and radial components of velocity, tip losses, and slipstream contraction were neglected. Each blade was replaced by a rotating lifting line. The trailing vortices which sprang from the tips formed a helix in space while the vortices from the root became concentric with the axis of rotation and were neglected. The problem thus was reduced to finding the normal component of the velocity which was induced at the rotor disk by a cylindrical surface of vorticity.

In order to simplify the analysis, the helical pattern of vorticity was broken up into two simpler patterns. One was composed of circular vortex rings and the other of axial vortex lines, both together forming a right circular cylinder of vorticity extending from the rotor disk downward to infinity. However in this analysis, the latter pattern was neglected. The analysis makes use of the fact that the potential Φ_p at a point P due to a closed vortex ring is directly proportional to the product of the circulation Γ' and the solid angle ω subtended by the vortex ring at P.

$$\Phi_p = \frac{\Gamma'}{4\pi}\omega$$

or using the differential equation for elementary vortex rings

$$d\Phi_p = \frac{\frac{d\Gamma}{dz}\, dz}{4\pi}\, \omega .$$

This equation was then integrated along the cylinder from $z = 0$ to ∞ and then differentiated for the induced velocity at the disk. It was then shown that for a constant circulation

$$v = -\frac{1}{2} \cdot \frac{d\Gamma}{dz} = \text{constant}$$

where $\frac{d\Gamma}{dz}$ is the circulation per unit length along the cylinder. It was also shown that the induced velocity in the plane of, but outside of the rotor disk was zero. Furthermore, it was shown that the velocity in the ultimate wake is

$$v_i = -\frac{d\Gamma}{dz}$$

thus corroborating the momentum result. By neglecting higher order infinitesimals and assuming a variation in circulation along the blade, it was shown that within the limitations of the assumptions, the independence of blade elements held.

These results were used to derive an expression for the inflow angle and hence to predict the lift and torque on a blade by means of the usual methods. The resulting thrust and torque equations compared favorably with experiment.

Knight and Hefner also made a somewhat similar analysis of a lifting airscrew in ground effect (reference 41). All the previous assumptions were assumed to hold except the independence of blade elements. An additional assumption was made in order to reach an approximate solution. This was that the circulation along the airscrew blades was constant; i.e., it was independent of both the blade radius and the distance above the ground plane. The vortex system was the same as in their previous paper, except that the vortex cylinder extended only to the ground plane. The effect of the ground plane was

28.

represented by placing a second cylindrical vortex sheet of equal length and strength but of opposite direction at the end of the first cylinder. Thus the second became a mirror image of the first.

The authors solved for the value of the induced velocity at the center of the rotor and at the tips and showed that the solution at other points was extremely difficult and tedious due to the presence of elliptic integrals of the third kind for which no tables were available. Methods of approximation were tried and Simpson's rule yielded satisfactory results for values of $\frac{x}{R} < 2$, except near the tips. For larger values of $\frac{x}{R}$ or as $x \rightarrow R$, this method required the computation of a prohibitive number of ordinates. It was then shown that the calculated results compared satisfactorily to the experimental data.

R. P. Coleman, A. M. Feingold, and C. W. Stempin utilized the vortex theory in their analysis (reference 42) of the longitudinal variation of the induced velocity across a rotor disk in forward flight. The study was undertaken in order to find a reasonable explanation for the vibration encountered by helicopters in slow speed forward flight. The simplified vortex system was also used as a conception of the rotor wake. In this instance the wake pattern was assumed to form an elliptic cylinder skewed with respect to the rotor axis at an angle depending upon the forward velocity and the induced velocities. It was also assumed that the rotor consisted of an infinite number of lightly loaded blades with constant circulation and that the helical vortex system could be replaced by a series of circular vortex rings whose plane remained parallel to the rotor disk, and a series of axial vortex lines.

In order to find the wake skew angle χ, the induced velocity components parallel and perpendicular to the wake axis were assumed to be constant. Then by taking the line integral of the velocity around suitable paths, it was shown

that the ratio of the induced velocity component perpendicular to the wake axis in the direction of forward flight to the induced velocity component parallel to the wake axis was equal to the tangent of half the wake angle.

By applying the Biot-Savart law, it was shown that the velocity distribution normal to the disk induced by the assumed vortex wake was given by a double integral equation. This equation was solved at the center of the disk and the value obtained was then shown to be the average across the fore-and-aft diameter. Furthermore, it was shown that this value was half the component of the ultimate wake induced velocity which was perpendicular to the rotor disk. The fore-and-aft rate of change of the induced velocity was found by differentiating within the integral sign and evaluating the resultant integrals at the center of the disk. It was found that

$$\dot{v}_o = v_o \tan \frac{\chi}{2}$$

where $\dot{v}_o$ = rate of change of induced velocity at the center of the disk, v_o = average value of fore-and-aft induced velocity at the center of the disk, and χ = the wake skew angle.

The results were combined with Glauert's theory of reference 28 and an expression was arrived at for the induced velocity at the center of the disk in terms of the flight velocity and required thrust. A comparison was made with some experimental data and the authors concluded that this comparison indicated that the most significant factors had been taken into account.

In reference 12, the results of this analysis were also compared with the experimentally determined induced velocities. In this case the measured values of the induced velocities at the center of the disk were somewhat lower than the calculated values for all three flight speeds. The experimentally determined slopes of the induced velocity variation were all higher than that yielded by

30.

the analysis. The theory appeared to yield a better comparison at the lower flight speeds. No definite conclusions were reached, however, since the experimental induced velocities were not determined for the fore-and-aft diameter, and since some lateral asymmetry was supposed to exist.

In reference 13, as stated in a previous section, large periodic forces were found to exist on rotor blades in forward flight which excited the first, second, and third bending modes of the rotor blades at frequencies of from three to ten times rotor frequency. As before an effort was made to theoretically predict these forces, and the linear downwash distribution of Coleman, Feingold, and Stempin was incorporated in the theory for finding the generalized forces. It was found that the loading terms which were directly affected by this type variation were the first harmonic cosine loading and the second harmonic sine loading. The remaining higher order harmonic loadings were proportional to blade flapping coefficients. It was shown that this linear induced velocity distribution had a minor effect on all blade flapping coefficients except the first harmonic sine coefficient. A comparison was made of the theoretical generalized forces and the test data. It was found that fair agreement was obtained at high tip speed ratios, but the analysis was not capable of explaining the peaks in the generalized forces in the transition region.

Drees (reference 43), by using the vortex concept of the lifting rotor, has developed a theory which is applicable to all flight conditions but was still limited to a great extent by the necessary assumptions for the solution of the problem. In his paper, the usual assumptions were made: i.e. contraction and rotation of slipstream was neglected, number of rotor blades was infinite, circulation was constant along the blade radius, and the angle between the slipstream and the rotor disk at each point of the disk was constant.

Although it was assumed that the circulation along the blade was constant, it was quite obvious that in forward flight, the circulation must vary with the azimuth angle ψ. It was then assumed that the circulation could be written as

$$\Gamma = \Gamma_0 - \Gamma_1 \sin\psi$$

Values of Γ_0 and Γ_1, were found by equating the constant portion of the lift to the weight and by setting the condition that the lift moment about the flapping hinge must be constant and independent of ψ. Then by neglecting second and higher harmonics it was shown that

$$\Gamma_0 = \frac{2W}{\rho b \Omega R^2 (1 - \frac{3}{2}\mu_v^2)}$$

$$\Gamma_1 = \frac{3}{2}\mu_v \Gamma_0$$

The axial velocity was taken as being composed of the following components: the component of the flight velocity perpendicular to the tip path plane; the component due to the bound vortices around the blades; the component from the free vortices moving with the slipstream and springing from the blade tips only, since Γ is assumed constant along the radius; and the component from the free radial vortices influencing the axial flow which compensates for the variation of Γ with respect to ψ. The induced velocities were calculated only for the X and Y axes at the 3/4 radius station and at the rotor center. A more accurate solution was considered impractical in use and not in accordance with the other simplifications. For performance calculations, a certain velocity distribution was assumed to exist through these points as a function of the radius and/or as a first harmonic function of the azimuth angle, ψ. Terms of higher than the first order were neglected.

The induced velocity of the bound vortices was arrived at by means of the following reasoning and by the usual mathematical solution for a finite vortex

32.

line. It was reasoned that, since Γ was symmetrical to the Y axis, it could have no influence on the axial velocity across a lateral diameter of the disk and, for the same reason, Γ_0 could have no influence on the axial velocity along the X axis or longitudinal diameter of the rotor disk. Thus only Γ_1 gave an axial induced velocity component along the X axis. The solution of the mathematical relationships involved complete elliptic integral equations. Assuming the component of the induced velocities due to the bound vortices to be a cosine function, these equations yielded for the 3/4 radius station

$$v''_{z_{\frac{3}{4}R}} = -0.6 \frac{b\Gamma_1}{2\pi R} \cos\psi .$$

The component of the induced velocity due to the Γ_0 circulation component of the free tip vortices was found in the usual manner by assuming that the shed vortices formed closed vortex rings parallel to the tip path plane. Two integral equations were arrived at for the velocities along the longitudinal and lateral rotor diameter, but the integration while possible, was very complicated. These equations were, however, integrated for the rotor center and yielded

$$v'''_{z_0} = \frac{b\Gamma_0}{2\pi R \mu_v} \cdot \frac{\sin \alpha_s}{2}$$

where α_s is the angle between the slipstream and the perpendicular to the tip-path plane. When the equations were solved for $\alpha_s = 0$, they yielded an axial induced velocity which was constant for each point of the rotor disk. This was in agreement with the results of previous papers, which showed that the assumption of constant circulation along the blades gave the ideal axial velocity distribution in hovering. The two integral equations were also numerically integrated for the 3/4 radius stations on both longitudinal and lateral diameters. Then assuming a cosine variation, the result was given as

$$v'''_{z_{\frac{3}{4}R}} = \frac{b\Gamma_0}{2\pi R \mu_v} \tan \alpha_s \left(\frac{\cos \alpha_s}{2} + P \cos\psi \right)$$

where

$$p \approx \frac{1 - \cos \alpha_s}{2 \tan \alpha_s}$$

or in another manner

$$v''''_{z_{\frac{3}{4}R}} = v''''_{z_0} + \frac{b \Gamma_0}{4\pi R \mu_v} (1 - \cos \alpha_s) \cos \psi$$

The determination of the axial induced velocity due to the free radial-vortices and tip-vortices was more difficult. Since Γ varied cyclicly, a free axial vortex of $\mp d\Gamma$ was released and the free tip vortex also varied $\pm d\Gamma$. These vortices formed a surface. Using these actual distributions of circulation resulted in a very complicated calculation for the component at the 3/4 radius station. In order to arrive at a solution, it was necessary to resort to a simple analogy. The radial and tip vortices were taken together and assumed to form two circular cylinders. That is, the actual circulation distribution was replaced by the vortex system of two hypothetical rotors. These rotors had their axis on the lateral diameter of the actual disk. The cylinder at $\psi = 90^\circ$ had a strength of $-\Gamma_1$, while the cylinder at $\psi = 270^\circ$ had a strength of $+\Gamma_1$. These systems compensate on the longitudinal diameter and hence cause no variation in the induced velocity. Then in a manner similar to that of the free constant tip-vortices, the induced velocity component at the 3/4 radius station and assuming a sine variation was shown to be

$$v''''_{z_{\frac{3}{4}R}} = -\frac{b \Gamma_1}{2\pi R \mu_v} \cdot \frac{\sin \alpha_s}{2} \sin \psi .$$

All the above components were added together to yield the total axial induced velocity. The equations were then non-dimensionalized but were not valid for ideal vertical autorotation when the airflow through the rotor disk approached zero. The theory was then changed in a semi-empirical manner to include this flight condition. A formula was arrived at which was valid for

34.

all flight conditions but had three constant coefficients which must be determined from flight and wind-tunnel tests. A correction for the deviation of the actual from the ideal uniform induced axial velocity was included. A chart was then presented which is valid for all kinds of one-rotor helicopters and autogyros and all normal speed combinations. The paper concluded with the equations for the determinations of α_1, the attitude angle of the fuselage and a_{1_s}, the angle between the rotor axis and the perpendicular to the tip-path-plane. Applications of the theory to several problems were given. Performance calculations were made for the Sikorsky S-51 and the theory predicted the experimental data to a good degree of accuracy.

W. Castles, Jr. and J. H. De Leeuw, in reference 44, presented a method for computing the approximate values of the normal component of the induced velocity at points in the flow field of a lifting rotor. In this paper the assumption was also made that the slipstream of the rotor could be considered as a uniform continuous distribution of vortex rings of infinitesimal strength. These rings were assumed to lie in planes parallel to the tip path plane and to form a straight elliptic cylinder extending from the disk to infinity. Then by using the stream function at a point P in the flow field of a vortex ring, expressions were arrived at for the axial and radial components of the induced velocity. These expressions were rather complicated since they involved the complete elliptic integrals of the first and second kinds and were given as follows:

$$V_z = \frac{\Gamma}{2\pi x R}(AB + CDF)$$

$$V_r = -\frac{\Gamma}{2\pi x R}(AB' + CDF')$$

where the terms within the brackets are functions of the complete elliptic integrals and non-dimensional distances of the point P from certain references. These terms are defined in the original paper.

It may be seen that the expressions become indeterminant for x = o (rotor center). It had been previously shown that for this case

$$(v_z)_{x=0} = -\frac{\Gamma}{2R}\left[\frac{1}{(1+z^2)^{3/2}}\right]$$

The above expressions were rewritten in non-dimensional form. The factor, $\frac{v_z R}{\Gamma}$ the non-dimensional normal component of the induced velocity in the vicinity of a vortex ring appeared on the left side of the expression and the right side of the expression became a function of the geometry of the problem; i.e. the distances of the point P from the center of the ring. Numerical values of this factor $\frac{v_z R}{\Gamma}$ were calculated and tabulated for various non-dimensional axial and radial distances from the center of the ring. The intervals were so chosen that numerical integration by Simpson's rule could be accomplished. Then using the resulting table, the normal component of induced velocity at a point P in the vicinity of a rotor whose wake was composed of these rings could be found by adding up the contributions of each vortex ring covered by the table. This would account for about 95% of the total induced velocity component at the center of the rotor and for a large part of the component for most points considered by the paper. The contribution of the rings outside the scope of the table were summed by using an approximate integral equation capable of solution which was said to introduce small error. Thus an expression was arrived at for the contributions of the vortex rings from the limits of the table to infinity. This expression was a function of the geometrical position of the point under consideration and the wake angle of the slip-stream at the rotor.

The results were presented in the form of tables and graphs of the ratio of the normal induced velocity component at point P to the normal component of induced velocity at the center of the rotor.

36.

A method was then given for the determination of the mean value of the normal component of induced velocity over the front and rear rotors of a tandem helicopter; for the determination of the longitudinal variation of the normal component of the induced velocity over the front and rear rotors of a tandem helicopter and for the determination of the induced flow angle at a horizontal tail plane.

In conclusion, the authors of the paper stated that for the high speed forward flight condition, the assumption that the vortex rings remain parallel to the tip path plane was the only one likely to affect the engineering accuracy of the results. Whereas for the slower speed case, the initial assumptions as to the vortex ring spacing and circulation distribution along the blades would affect the accuracy of the calculations. They therefore advised exercising caution in applying the theory to points on or close to the disk of a specific rotor at low forward flight velocities. No comparison with experiment was made.

Flow Visualization Studies

There have been many experimental investigations which have studied the air flow through and around both propellers and helicopters. Most of these have dealt with models, though a few have used full scale helicopters under actual flight conditions. The purpose was to gain a more accurate knowledge of the flows, with the thought that if the actual flow were understood, perhaps the theory could be improved either by incorporating simplifying assumptions in the mathematics or by devising an empirical method. The results were also used as a check on the applicability of existing theories.

There have been four methods of flow visualization employed: cotton tufts, smoke, balsa dust, and hot wire and spark shadowgraphs. From the available experimental results, the following general conclusions may be drawn. Of the four, the cotton tufts seem to be of least value, since they suffer a great deal from gravity and flutter, particularly in the rotor wake. Smoke photographs appear to yield better results for streamline study, while balsa-dust photographs appear to yield a better overall picture of the flow. The hot wire and spark shadowgraphs appear to be the better method for studying vortex and wake helix patterns because the heated filaments of air do not appear to dissipate too quickly. Some examples of these methods as applied to propellers and rotors are reviewed in the following paragraphs.

Lock and Townend, in reference 45, investigated the flow around a model propeller working in water in the "vortex ring state." The model propeller was of extremely small scale having a diameter of one inch. Ten photographs were presented including views of the flow conditions from the normal working state through the static thrust condition to the vortex ring and windmill brake state. Lock, in reference 46, repeated these tests using a three foot

38.

diameter airscrew in a windtunnel with cotton tufts as the means for flow visualization. Twelve photographs were presented covering the various states as listed above. The photographs clearly showed the extreme turbulence which exists about an airscrew in the vortex ring state.

Townend, in reference 47, used hot wire and spark shadowgraphs in a study of the periodic airflow through a propeller. The use of the spark shadowgraphs enabled the velocity and the direction of flow to be mapped out. The shadowgraphs of the hot wire tests very clearly showed the radial flow that exists in the slipstream. The heated air filaments were broken by the blade and this break passed downstream as a discontinuity, the particle that passed just under the blade moved outward while the adjacent particle which had passed just over the blade moved inward. This discontinuity represented the helicoidal vortex sheet left behind by the blade. The filaments also very clearly showed the tip vortices which were shed and their spacing. The centers of these "eddies" as they appeared in the shadowgraphs represented the slipstream boundary. The heated dots formed by the injected sparks were introduced near the blade tips. The resulting shadowgraphs showed very clearly the formation of the trailing tip vortices. The high velocities which existed in this region were indicated by the elongation of the dot shadows. These photographs are an excellent though brief study of the periodic flow existing behind an airscrew.

Brotherhood, in references 48 and 49, and Brotherhood and Stewart, in reference 12, investigated the air-flow through a full scale helicopter rotor in various free flight conditions. Velocity measurements were made and pictures were taken of the various flow patterns formed by smoke streamers. Reference 48 is an investigation of the air-flow through a helicopter rotor when hovering both in and out of ground effect. The smoke visualization of the streamlines

was used to refer back to their appropriate disk positions the velocity measurements which were taken in the fully developed slipstream. The experimental measurements agreed very well with that predicted by propeller strip theory of reference 1, if tip losses were taken into account. The smoke filaments gave a good indication of the streamline pattern in the slipstream. Reference 49 was an investigation of the air-flow through a rotor in vertical descent. Smoke filaments were introduced below the rotor at several radii. The pictures of the smoke pattern in vertical descent clearly indicated the various types of flow associated with the rotor as it passed through the vortex-ring state into the windmill-brake state of operation. There was very good agreement between the rates of descent corresponding to autorotation as obtained from the smoke photographs and from power considerations. Reference 12 has been previously discussed. It presented smoke photographs of the flow through a rotor in forward flight. The helicopter was flown behind an aircraft which was trailing smoke generators suspended from a long wire. The smoke trails passed through the rotor and were photographed from the side by another aircraft. The resulting photographs indicated the increase in induced velocity from the front to the rear of the disk. The results were in reasonable agreement with theoretical predictions.

Taylor, in reference 50, developed and illustrated a balsa-dust technique for the visualization of air-flow patterns through model helicopter rotors both in steady-state and transient-flow conditions. Some very striking photographs were obtained, particularly of the starting vortex shed from the blade tips while the rotor was brought up to speed from rest, both for single and coaxial rotor configurations. Photographs were also given of single, coaxial, and biaxial (with varying degrees of overlap) rotor configurations in and out of ground effect. This method illustrated the overall flow picture very well.

40.

Drees and Hendal, in reference 51, photographed the flow of smoke filaments through and around a model helicopter mounted in a wind tunnel under various flight conditions. A method was devised for introducing smoke at the exact local velocity. The smoke could be turned on and off instantaneously, was non-corrosive, and was easily regulated. Photographs of the smoke flow were made for hovering flight and various rates of vertical descent through the vortex-ring state into the windmill-brake state. In general the turbulence was so great as to completely dissipate the smoke filaments after they had passed through the rotor. An interesting series of photographs showed a marked periodicity of airflow pattern for descending flight at low forward speed, the helicopter being in the vortex-ring state. This corresponds to the region of roughness. The model helicopter rotor was observed to "tumble" regularly with the same period as the shedding of the vortex ring. At higher forward speeds, the phenomenon disappeared. For autorotation in forward flight, the photographs showed that there was up flow in the front part of the disk, but that near the rear, there was a region of downflow.

Meyer and Falabella, in reference 52, have measured the aerodynamic loading on a model helicopter blade in forward flight by recording the pressure variations by means of pressure taps, positioned both spanwise and chordwise on the blade. The results have been plotted as curves of constant aerodynamic loading versus position on the rotor disk. This reference would yield excellent data for checking any future theory.

Discussion

As may be seen from the reviews presented in the preceeding sections, simplifications of the physical picture were necessary in order to obtain solutions for the induced velocity field. These assumptions and their effects will be discussed below.

The primary and perhaps the most universal assumption is that the rotor is made up of an infinite number of blades. In the vortex theory this implies zero slipstream contraction since the resulting wake boundary may then be taken as a cylindrical sheet of vorticity for which there can be no radial flow within the wake. In these cases the additional assumptions are usually made that the circulation along the blades is constant and that the effect of the vortices shed off the blade root may be neglected except insofar as it results in a rotational component of induced velocity about the wake axis. In the momentum theory, this assumption implies that the rotor may be replaced by a pressure step, the distribution of which must either be assumed or solved for with the aid of other simplifying assumptions while the velocity remains continuous through the disk. An extension of this concept is that of the actuator disk in which the rotor is replaced by a pair of infinitely bladed, contra-rotating tandem rotors so designed that the rotational component of induced velocity of the front rotor is exactly cancelled by the rear rotor. The result of the assumption of an infinite number of blades yields an induced velocity variation which is not periodic. For fast-moving multi-bladed propellers and rotors this would appear to be a good assumption but for large-diameter, slow-moving rotors with only one or several blades, the assumption would appear to be rather poor even for performance estimation.

The second usual assumption is that the blades are lightly loaded. This may also imply several things. One is that the slipstream contraction may again be

42.

neglected which means that the inflow velocity must be very small compared to the rotational velocity component of the blade section. Another is that in forward flight, the velocity along the flight path is large compared to the induced velocities and hence the theory may be linearized. This assumption may result in a reasonable approximation if care is taken in interpreting the limitation of smallness. At present this limitation is not clearly defined.

The assumptions that the slipstream contraction and rotation may be neglected while in error physically appear to have little or no effect on the results of the vortex theory as compared to performance data. However, the former is obviously incompatible with the momentum theory while the latter probably has a small effect.

The assumption of a constant circulation along the blade span axis has been a necessary assumption in most vortex theories. (The exception being Goldstein's theory.) This distribution is theoretically obtainable by the proper twist and/or taper of the blade but this is not practicable. In practice the actual circulation distribution is quite different from the assumed constant value.

It has been shown experimentally by Lock in reference 20 that the assumption of the independence of blade elements in the blade element theories is a reasonable approximation and yields good results.

Goldstein's theory in reference 37 and as modified by Lock in reference 38 employed only one of the assumptions stated above which was that the blades must be lightly loaded, though this later was shown to be an unnecessary condition. The basic assumption of the theory was that the wake was pictured as composed of a rigid helicoidal surface (or co-axial surfaces) of infinite length but finite radius moving with a uniform axial velocity which was small compared to the rotor blade tip speed. Then the velocity field of the vortex system at a

great distance behind the rotor was equivalent to the potential field of these rigid helicoidal surfaces. The conditions existing in the wake were then related to the rotor planform. The solution is, however, only rigorously correct for rotors whose distribution of circulation along the blades will yield a flow in the wake that is identical with the potential flow of such a set of rigid equidistant co-axial helicoidal surfaces. It appears that the theory may be applied with small error to the general case of a hovering or vertically ascending rotor. This is the only theory, with the exception of Prandtl's tip loss correction (reference 36), that takes into account the interference effects of a finite number of blades.

In all cases the working medium was assumed to be an incompressible, inviscid gas.

In the main, these assumptions which have been discussed appear to be reasonably well founded because the resulting performance theory predicts the overall experimental data to a good degree of accuracy. However, when these theories are applied to the calculation of the dynamic air loadings on the blade for blade motion, vibration, and stress analyses, it becomes apparent that they are woefully inadequate (for instance, the efforts of Doughaday and Kline in reference 13). It would therefore appear to be worthwhile to attempt to extend the present theories or to find another solution to the problem which is not as greatly limited in its applicability. One of the primary objectives of such an attempt would be the incorporation of the effect of the periodicity of flow and the interference effects of a small number of blades. The neglect of these effects may be the cause of the major discrepancies appearing in the present theories.

The search for a general solution has been almost completely thwarted by the lack of suitable mathematical tools. This deficiency has made it necessary

44.

to so simplify the true physical picture that many of the practical uses which could have been derived from the results have largely been lost. It is obvious from the reviewed papers that men of stature have grappled with the problem and have met only limited success, not through lack of effort or intelligence, but because of the limits of mathematical knowledge. The author of this paper does not presume to have the ability to extend these mathematical limits. However, with these thoughts in mind, a program of investigation has been laid out which should result in some further degree of success.

It would seem that the possibility of practically extending the knowledge by using the mathematical artifices and physical simplifications of the reviewed papers have been largely exhausted. Further advances along these lines would appear to require prohibitive amounts of graphical integrations or numerical calculations though electronic computers may make this approach feasible.

It is therefore proposed that a search for a solution be instituted which will be guided along two lines of endeavor. The first of these would be a systematic search of the more recent papers and journals in the fields of mathematics and the physical sciences for a new or different mathematical method or artifice. The second approach would be a flow visualization study of the velocity field about a helicopter rotor in the various flight conditions. The purposes of the latter study would be to indicate what simplifications may be made which would not too greatly limit the applicability of a solution to practical problems. It is thought that these two methods of approach would offer some hope of finding a more satisfactory solution to the problem of the induced velocity field about a helicopter rotor.

Conclusions & Recommendations

The rotor induced velocity field theories that have been reviewed herein have made definite and worthwhile contributions to the understanding of the flow through helicopter rotors. However they have in the main been either over-simplified, limited by their assumptions to special flight conditions, or are rather long and tedious in application. In general the problem of the periodicity of flow has been neglected entirely. It is therefore recommended that a program of study be initiated which will be directed toward finding a more practicable solution to the problem of the induced velocity field about a helicopter rotor.

46.

References

1. Durand, W. F.: Aerodynamic Theory. 1st ed., vol. IV, Julius Springer, Berlin, 1935.

2. Gessow, Alfred: Standard Symbols for Helicopters. NACA TN 1604, June 1948.

3. Rankine, W. J. M.: On the Mechanical Principles of the Action of Propellers. Transactions Institute of Naval Architects, vol. 6, p.p. 13-39, 1865.

4. Froude, R. E.: On the Part Played in Propulsion by Differences of Fluid Pressure. Trans. Inst. Naval Arch., vol. 30, p. 390, 1889.

5. Joukowski, N. E.: Travaux du Bureau des Calculs et Essais Aéronautiques de l 'Ecole Superièure Technique de Moscou, 1918; republished in book form as Théorie Tourbillonnaire de l'hélice Propulsive, Paris, 1929.

6. Betz, A.: Eine Erweiterung der Schraubenstrahltheorie, Zeitschrift für Flugtechnik und Motorluftschiffahrt, 11, 105, 1920.

7. Mangler, K. W. and Squire, H. B.: The Induced Velocity Field of a Rotor. British ARC R&M No. 2642, May 1950.

8. Mangler, K. W.: Calculation of the Induced Velocity Field of a Rotor. British RAE Report No. Aero. 2247, Feb. 1948.

9. Mangler, K. W.: Fourier Coefficients for Downwash at a Helicopter Rotor. British RAE Tech. Note No. Aero. 1958, May 1948.

10. Durand, W. F.: Aerodynamic Theory. 1st ed., vol. II, Julius Springer, Berlin, 1935.

11. Kinner, W.: Die kreisfoermige Tragflaeche auf potentialtheoretischer Grundlage. Ingenieur Archiv. vol. VIII, p.p. 47-80, 1937. The Principle of the Potential Theory Applied to the Circular Wing. R.T.P. Translation No. 2345 issued by the Ministry of Aircraft Production, (British).

12. Brotherhood, P. and Stewart, W.: An Experimental Investigation of the Flow Through a Helicopter Rotor in Forward Flight. British ARC R&M 2734, Sept. 1949.

13. Daughaday, H. and Kline, J.: An Approach to the Determination of Higher Harmonic Rotor Blade Stresses. Proceedings of the Ninth Annual Forum, American Helicopter Society, Inc., May 14, 15, 16, 17, 1953, p.p. 90-126.

14. Fail, R. A. and Eyre, R. C. W.: Downwash Measurements Behind a 12 ft. Diameter Helicopter Rotor in the 24 ft. Wind Tunnel. British R.A.E. Tech Note Aero. 2018, Sept. 1949. (RESTRICTED)

15. Froude, W.: On the Elementary Relation Between Pitch, Slip, and Propulsive Efficiency. Trans. Inst. Naval Arch; vol. 19, p.p. 47-65, 1878.

16. Drzewiecki, S.: Bulletin del 'Association Technique Maritime. 1892, et seq.

17. Drzewiecki, S.: Des hélices aériennes théorie générale des propulseurs Paris, 1909.

18. Drzewiecki, S.: Théorie générale de l'hélice. Paris, 1920.

19. Lanchester, F. W.: Aerodynamics. Constable & Co., Ltd., London, 1907.

20. Lock, C. N. H.: Experiments to Verify the Independence of the Elements of an Airscrew Blade. British R&M 953, 1924.

21. Reissner, H.: Z.F.M. 1, 257, 309; 1910.

22. Betz, A.: Die wichtigsten Grundlagen für den Entwurf von Luftschrauben. Z.F.M. 6, 97, 1915.

23. de Bothezat, G.: The General Theory of Blade Screws. NACA TR 29, 1918.

24. Fage, A. and Collins, H. E.: An Investigation of the Magnitude of the Inflow Velocity of the Air in the Immediate Vicinity of an Airscrew, with a View to an Improvement in the Accuracy of Prediction from Aerofoil Data of the Performance of an Airscrew. British ARC R&M 328, 1917.

25. Bairstow, L.: Applied Aerodynamics, London, 1919.

26. Wood, R. McK. and Glauert, H.: Preliminary Investigation of Multiplane Interference Applied to Propeller Theory. British ARC R&M 620, 1918.

27. Glauert, H.: An Aerodynamic Theory of the Airscrew. British ARC R&M 786, 1922.

28. Glauert, H.: A General Theory of the Autogyro. British ARC R&M 1111, 1926.

29. Glauert, H. Vertical Ascent of a Helicopter. British ARC R&M 1132, 1927.

30. Glauert, H, Horizontal Flight of a Helicopter. British ARC R&M 1157, 1928.

31. Lock, C.N.H.: Further Development of Autogyro Theory. British ARC R&M 1127, 1927.

32. Squire, M. A.: The Flight of a Helicopter. British ARC R&M 1730, 1935.

33. Ross, Robert S.: An Investigation of the Airflow Underneath Helicopter Rotors. Journal of the Aeronautical Sciences, vol. 13, No. 12, p.p. 665-677, Dec. 1946.

48.

34. Castles, Walter and Ducoffe, Arnold L.: Static Thrust Analysis for Helicopter Rotors and Airplane Propellers, Journal of Aeronautical Sciences, vol. 15, No. 5, p.p. 293-299, May 1948.

35. Margoulis, W.: Propeller Theory of Professor Joukowski and his Pupils. NACA TM 79, April 1922.

36. Betz, A.: Schraubenpropeller mit geringstem Energieverlust. Göttinger Nachr, p. 193, 1919.

37. Goldstein, S.: On the Vortex Theory of Screw Propellers. Proc. Roy, Soc. (London), ser. A. vol. 123, No. 792, p.p. 440-465, April 6, 1929.

38. Lock, C.N.H.: Application of Goldstein's Airscrew Theory to Design. British ARC R&M 1377, Nov. 1930.

39. Nikolsky, A. A.: Helicopter Analysis. John Wiley & Sons, Inc. New York, 1951, p.p. 17-21.

40. Knight, Montgomery and Hefner, Ralph A.: Static Thrust Analysis of the Lifting Airscrew. NACA TN 626, Dec. 1937.

41. Knight, Montgomery and Hefner, Ralph A.: Analysis of Ground Effect on the Lifting Airscrew. NACA TN 835, Dec. 1941.

42. Coleman, Robert P., Feingold, Arnold M. and Stempin, Carl W.: Evaluation of the Induced Velocity Field of an Idealized Helicopter Rotor. NACA ARR/L5E10/WRL-126.

43. Drees, Meijer, A Theory of Airflow Through Rotors and its Application to Some Helicopter Problems. The Journal of the Helicopter Association of Great Britain, vol. 3, No. 2, July-Aug.-Sept. 1949, p.p. 79-104.

44. Castles, Walter, Jr., and De Leeuw, Jacob Henri: The Normal Component of the Induced Velocity in the Vicinity of a Lifting Rotor and Some Examples of its Application. NACA TN 2912, March 1953.

45. Lock, C. N. H. and Townend, H. C. H.: Photographs of the Flow Round a Model Screw Working in Water, Especially in the "Vortex Ring State." British ARC R&M 1043, May 1926.

46. Lock, C. N. H.: Photographs of Steamers Illustrating the Flow Around an Airscrew in the Vortex Ring State. British ARC R&M 1167, April 1928.

47. Townend, H. C. H.: Hot Wire and Spark Shadowgraphs of the Airflow Through an Airscrew. British ARC R&M 1434, Sept. 1931.

48. Brotherhood, P.: An Investigation in Flight of the Induced Velocity Distribution under a Helicopter Rotor when Hovering. British ARC R&M 2521, June 1947.

49. Brotherhood, P.: Flow Through a Helicopter Rotor in Vertical Descent. British ARC R&M 2735, July 1949.

50. Taylor, Marion K.: A Balsa-Dust Technique for Air-Flow Visualization and its Application to Flow Through Model Helicopter Rotors in Static Thrust. NACA TN 2220, Nov. 1950.

51. Drees, Meijer and Hendal, W. P.: Airflow Patterns in the Neighborhood of Helicopter Rotors. Aircraft Engineering, vol. XXIII, No. 266, p.p. 107-111, April 1951.

52. Meyer, John R. Jr. and Falabella, Gaetano, Jr.: An Investigation of the Experimental Aerodynamic Loading on a Model Helicopter Rotor Blade, NACA TN 2953, May 1953.

HELICOPTER DISTRIBUTION LIST

INDUSTRY

1. Gyrodyne Corporation of America
   Flowerfield
   St. James, Long Island, New York

   via: Office of Naval Research Branch Office
   346 Broadway
   New York 13, N. Y.

2. McDonnell Aircraft Corporation
   St. Louis, Missouri

3. Bell Aircraft Corporation
   Helicopter Division
   P. O. Box 482
   Ft. Worth 1, Texas

4. Sikorsky Aircraft Division
   United Aircraft Corporation
   Bridgeport, Connecticut

5. Kaman Aircraft Corporation
   Bradley Field
   Windsor Locks, Connecticut

   ATTENTION: Vice President-Engineering

6. Kellett Aircraft Corporation
   P. O. Box 468
   Camden 1, New Jersey

7. Doman Helicopters, Inc.
   Municipal Airport
   Danbury, Connecticut

   ATTENTION: Chief Design Engineer

   via: Inspector of Naval Material
   1285 Boston Ave.
   Bldg. 23C
   Bridgeport 8, Connecticut

8. American Helicopter Company, Inc.
   3613 Aviation Blvd.
   Manhattan Beach, California

9. Rotor Craft Corporation
   1850 Victory Blvd.
   Glendale 1, California

10. Piasecki Helicopter Corporation
Morton, Pennsylvania

ATTENTION: Chief of Research

11. Goodyear Aircraft Corporation
Akron, Ohio

ATTENTION: Research & Development
D/20 Plant C

12. Helicopter Division
Hughes Aircraft Company
Culver City, California

13. McCulloch Motors
Aircraft Division
9775 Airport Blvd.
Los Angeles, California

14. Hiller Helicopters
Palo Alto, California

15. Flettner Aircraft Corporation
c/o Milco Eng. Company
520 Morgan Avenue
Brooklyn 22, New York

16. Helicopter Division
Cessna Aircraft Company
Wichita, Kansas

17. E. Gluhareff Helicopters, Inc.
1050 Duncan Place
Manhattan Beach, California

via: Inspector of Naval Material
1206 South Santee St.
Los Angeles 15, California

18. Jacobs Aircraft Engine Co.
Pottstown, Pa.

ATTENTION: Chief Development Engineer

19. J. B. Rea Company, Inc.
11941 Wilshire Blvd.
Los Angeles 25, California

20. Minneapolis-Honeywell Regulator Company
Aeronautical Division
2600 Ridgway Road
Minneapolis 13, Minnesota

21. Flight Control Department, P-32
Sperry Gyroscope Company
Great Neck, New York

22. Lear Inc.
11916 West Pico Blvd.
Los Angeles 64, California

via: Inspector of Naval Material
1206 South Santee St.
Los Angeles 15, California

23. Department of Aeronautical Engineering
The James Forrestal Research Center
Princeton, New Jersey

(5 copies)

24. Cornell Aeronautical Laboratory, Inc.
4455 Genesee Street
Buffalo 21, New York

ATTENTION: Helicopter Research Section

25. Director, Guggenheim School of Aeronautics
Georgia Institute of Technology
Atlanta, Georgia

26. Department of Aeronautical Engineering
Massachusetts Institute of Technology
Cambridge, Massachusetts

via: Office of Naval Research Branch Office
150 Causeway St.
Boston 14, Mass.

GOVERNMENT

1. Office of Naval Research
Department of the Navy
Washington 25, D. C.

ATTENTION: Code 461

(8 copies)

2. Office of Naval Research
Special Devices Center, Code 910
Port Washington, New York

3. Office of Naval Research Branch Office
American Fore Building
844 North Rush Street
Chicago 11, Illinois

4. Director, Naval Research Laboratory
Washington 25, D. C.

ATTENTION: Technical Information Officer

5. Office of the Asst. Naval Attache for Research
Naval Attache
American Embassy
Navy 100
FPO New York, New York

6. Office of Naval Research Branch Office
346 Broadway
New York 13, New York

7. Office of Naval Research Branch Office
1030 East Green Street
Pasadena 1, California

8. Office of Naval Research Branch Office
1000 Geary Street
San Francisco 9, California

9. Bureau of Aeronautics
Department of the Navy
Washington 25, D. C.

ATTENTION: AC-4

10. Bureau of Aeronautics

ATTENTION: DE-32

11. Bureau of Aeronautics

ATTENTION: RS-91

12. Bureau of Aeronautics

ATTENTION: AE-731

13. Bureau of Aeronautics

ATTENTION: TD-412

14. Aeronautical Instruments Laboratory
Naval Air Material Center
Philadelphia, Pennsylvania

15. Wright Air Development Center
Wright-Patterson Air Force Base
Dayton, Ohio

ATTENTION: WCOWR

(2 Copies)

16. Rotary Wing Branch
Flight Test Division
Naval Air Test Center
Patuxent River, Maryland

(2 Copies)

17. Office Chief of Transportation
Department of the Army
Washington 25, D. C.

ATTENTION: TCATS - Engineering and Development

18. Flight Test Branch
Aircraft Engineering Division
Civil Aeronautics Administration, Code W-303
Washington 25, D. C.

19. National Advisory Committee for Aeronautics
1724 "F" Street, N. W.
Washington 25, D. C.

(2 Copies)

20. Aviation Department
Westinghouse Electric Corp.
1625 K St. N.W.
Washington, D. C.

ATTENTION: Mr. J. O. Fassett

21. Bureau of Aeronautics
Department of the Navy
Washington 25, D. C.

ATTENTION: DE-31

22. Aerodynamics Laboratory
The David Taylor Model Basin
Washington 7, D. C.

23. ASTIA Document Service Center
Knott Building
Dayton 2, Ohio

(3 Copies)